**In situ detection of methylated DNA by histo endonuclease-linked detection of methylated DNA sites: a new principle of analysis of DNA methylation**

Takehiko KOJI, Shiho KONDO, Yoshitaka HISHIKAWA, Shucai AN and Yoko SATO

Department of Histology and Cell Biology, Nagasaki University Graduate School of Biomedical Sciences, Sakamoto, Nagasaki 852-8523, Japan

*Running Title:* A new method for DNA methylation analysis

*Correspondence to:* Prof. Takehiko Koji, Department of Histology and Cell Biology, Nagasaki University Graduate School of Biomedical Sciences, 1-12-4 Sakamoto, Nagasaki 852-8523, Japan.

Phone: +81-95-819-7025, Fax: +81-95-819-7028

e-mail: tkoji@nagasaki-u.ac.jp

**Abstract**

For a better understanding of epigenetic regulation of cell differentiation, it is important to analyze DNA methylation at a specific site. Although previous studies described methylation of isolated DNA extracted from cells and tissues using a combination of appropriate restriction endonucleases, no application to tissue cell level has been reported. Here, we report a new method, named histo endonuclease-linked detection of methylation sites of DNA (HELMET), designed to detect methylation sites of DNA with a specific sequences in a tissue section. In this study, we examined changes in the methylation level of CCGG sites during spermatogenesis in paraffin-embedded sections of mouse testis. In principle, the 3'-OH ends of DNA strand breaks in a section were firstly labeled with a mixture of dideoxynucleotides by terminal deoxynucleotidyl transferase (TdT), not to be further elongated by TdT. Then the section was digested with *Hpa* II, resulting in cutting the center portion of non-methylated CCGG. The cutting sites were labeled with biotin-16-dUTP by TdT. Next, the section was treated with *Msp* I, which can cut the CCGG sequence irrespective of the presence or absence of methylation of the second cytosine, and the cutting sites were labeled with digoxigenin-11-dUTP by TdT. Finally, both biotin and digoxigenin were visualized by enzyme- or fluorescence-immunohistochemistry. Using this method, we found hypermethylation of CCGG sites in most of the germ cells although non-methylated CCGG were colocalized in elongated spermatids. Interestingly, some TUNEL-positive germ cells, which are frequent in mammalian spermatogenesis, became markedly *Hpa* II-reactive, indicating that the CCGG sites may be demethylated during apoptosis.

**Introduction**

DNA methylation is involved in the maintenance of normal spermatogenesis in mammals. The methylation marks are erased in primordial germ cells, and the germ cell DNA is remethylated after sex determination in a sex-specific manner (Reik et al. 2001; Yamazaki et al. 2003; Li et al. 2004). DNA methylation occurs in mammals at cytosine residues in CpG sequence. However, CpG islands are generally devoid of methylation. The rest of the genome is highly methylated; the methylation state of non-CpG-island DNA correlates negatively with the regional level of GC contents in somatic tissues whereas the low-GC content regions are specifically hypomethylated in the testes (Oakes et al. 2007).

Mammalian spermatogenesis is an orderly arranged process consisting of spermatogonial proliferation, spermatocytic meiosis and spermiogenesis (Bellve et al. 1977). On the other hand, spermatogenesis can be also considered a process that serves to condense euchromatin to a completely packed heterochromatin in step-by-step germ cell differentiation (Koji & Hishikawa 2003). During spermatogenesis, germ cell death is very common; indeed, 25-75% of the expected sperm yield is thought to be lost (Oakberg 1956; Huckins 1978; Johnson et al. 1983). In rats and mice, the mode of germ cell death is almost of apoptotic nature (Allan et al. 1992; Wang et al. 1998) and mitochondrial death signals are involved in the induction of autonomous cell death in normal spermatogenesis (Koji & Hishikawa 2003).

Several lines of evidence suggest that the state of DNA methylation plays important roles in spermatogenesis. Kelly et al. (2003) reported that the use of

5-aza-2'-deoxycytidine, a cytidine analogue known to decrease the level of DNA methylation, results in histological anomalies in testis. Moreover, DNA methyltransferase-like protein (Dnmt3L) homozygous mutant mice, which exhibit low methylation of DNA in testis, are infertile (Bourc'his et al. 2001; Hata et al. 2002) and are subject to meiotic aberrations with the appearance of apoptosis-like germ cells (Bourc'his and Bestor 2004; Hata et al. 2006).

Considering that DNA methylation is closely related to chromatin condensation, we hypothesized that any abnormality of DNA methylation would result in the induction of apoptosis possibly due to ill-organized heterochromatinization. To correlate the state of DNA methylation with apoptotic germ cells, histochemical approach would be appropriate. In fact, an antibody against 5-methylcytosine is available and we can analyze the methylation state of DNA immunohistochemically in individual cells. However, the number of possible methylation sites (CpG) is too large and the data of immunohistochemistry cannot be correlated to the specific sequences of DNA.

Therefore, we attempted to develop a new histochemical method, histo endonuclease-linked detection of methylated DNA sites (HELMET), to assess the DNA methylation level at a specific site such as a CCGG sequence, using a set of restriction enzymes of methylation sensitive (*Hpa* II)- and insensitive (*Msp* I)-isoschizomers (Anway et al. 2005) on a histological section. The results revealed that during germ cell apoptosis, DNA demethylation proceeded and methylation levels of CCGG sites varied according to the differentiation stage of spermatogenic cells.

**Materials and Methods**

*Chemicals and biochemicals:*

Paraformaldehyde (PFA) was purchased from Merck (Darmstadt, Germany), and 3, 3'-diaminobenzidine 4HCl (DAB) was purchased from Dojin Chemical Co. (Kumamoto, Japan). Bovine serum albumin (BSA) (essentially fatty acid and globulin-free) and Trizma base and Brij-35 were from Sigma Chemical Co. (St. Louis, MO, USA). Biotin-16-dUTP, digoxigenin-11-dUTP and terminal deoxynucleotidyl transferase (TdT) were from Roche Diagnostics (Mannheim, Germany). +Dideoxy ATP (ddATP) and dideoxy TTP (ddTTP) were from Jena Bioscience (Jena, Germany). *Hpa* II and *Msp* I were purchased from Takara Bio Inc. (Shiga, Japan). Permount was purchased from Fisher Scientific Inc. (NJ, USA). All other reagents used in this study were from Wako Pure Chemicals (Osaka, Japan) and were of analytical grade.

*Antibodies*

Mouse monoclonal anti-5-methylcytosine (2.5 μg/ml) was purchased from Calbiochem (San Diego, CA, USA). Normal goat IgG and sheep IgG were purchased from Dako (Glostrup, Denmark). Horseradish peroxidase (HRP)-conjugated goat anti-mouse IgG (1: 100), HRP-conjugated goat anti-biotin (1: 100) and HRP-conjugated sheep anti-digoxigenin (1: 100) were from Chemicon International Inc. (Temecula, CA, USA). FITC-labeled goat anti-biotin (1: 100) was from Vector Laboratories (Burlingame, CA, USA) and rhodamine-labeled sheep anti-digoxigenin (1: 100) was from Roche Diagnostics (Mannheim, Germany).

*Animals and tissue preparation:*

Male adult ICR mice (8 to 10-week-old) weighing 27-38 g were used in the present study. Some of the mice were injected four times with diethylstilbestrol (DES) dissolved in corn oil at 20 mg/kg body weight every 5 days to induce germ cell apoptosis (Koji et al. 2001). Mice were sacrificed at 20 days-treatment with DES or vehicle alone. The experimental protocol was approved by the Animal Ethics Review Committee of Nagasaki University (#0112100012 and #0202200048).

The testes dissected out were cut into small pieces, then fixed overnight with 4% PFA in phosphate buffered saline (PBS) at 4°C and embedded in paraffin in a standard manner. Several serial sections were stained with hematoxylin and eosin (H&E), and used for identification of seminiferous epithelial cycles and the differentiation stages of germ cells.

*Immunohistochemistry for 5-methylcytosine:*

Immunohistochemical detection of 5-methylcytosine was performed on the paraffin sections of mouse testis, as described in detail previously (Matsuo et al. 2007). After they were dewaxed, the sections were immersed in 10 mM citrate buffer, pH 6.0, autoclaved at 120°C for 15 min, and then preincubated with 500 μg/ml normal goat IgG dissolved in 1% BSA in PBS, pH 7.2, for 1 h. Unless otherwise specified, all reactions were conducted at room temperature (RT). Then the sections were reacted overnight with anti-5-methylcytosine (2.5 μg/ml) in 1% BSA in PBS. After washing with 0.075% Brij in PBS three times for 15 min each, HRP-conjugated goat

anti-mouse IgG dissolved in 1% BSA in PBS was reacted for 1 h. After washing with

0.075% Brij in PBS three times for 15 min each, the sites of HRP were visualized

with DAB and $H_2O_2$ in the presence of nickel and cobalt ions (Shukuwa et al. 2006).

As a negative control, some sections were reacted with normal mouse IgG instead of

the specific monoclonal antibody.

*Terminal deoxynucleotidyl transferase-mediated dUTP nick end-labeling (TUNEL)*
*staining:*

To identify apoptotic germ cells, TUNEL was performed according to the method of

Gavrieli et al. (1992) with a slight modification (Koji et al. 2001; An et al. 2005).

Paraffin sections (5 to 6-μm thick) on silane-coated glass slides were dewaxed and

digested with 10 μg/ml of proteinase K in PBS at 37°C for 15 min. Then the sections

were incubated with TdT buffer (25 mM Tris/HCl buffer, pH 6.6, containing 0.2 M

potassium cacodylate and 0.25 mg/ml BSA) alone at RT for 30 min. After the

incubation, the slides were reacted with 800 units/ml of TdT dissolved in TdT buffer

supplemented with 0.5 μM biotin-16-dUTP, 20 μM dATP, 1.5 mM $CoCl_2$ and 0.1

mM dithiothreitol at 37°C for 90 min. As a negative control, TdT reaction was

conducted with 0.5 μM TTP instead of biotin-16-dUTP, or without TdT. After

washing with milli-Q water (Millipore, Molsheim, France) (DDW), the signals were

detected immunohistochemically with HRP-conjugated goat anti-biotin antibody or

FITC-labeled goat anti-biotin antibody. The sites of HRP were visualized by a mixture

of DAB, hydrogen peroxide, nickel and cobalt ions, as described above.

*HELMET:*

First, TdT reaction was conducted as described above on paraffin sections of mouse testis at 37°C for 2 h, except for the presence of 20 μM ddATP and 20 μM ddTTP instead of dATP and biotin-16-dUTP, to block the free 3'-OH ends of DNA. After washing with DDW and PBS, successively, the sections were fixed with 4% PFA in PBS for 5 min and then washed twice with PBS and once with DDW for 5 min each. Then the sections were reacted with 100 units/ml of *Hpa* II dissolved in 10 mM Tris/HCl buffer, pH 7.5, containing 10 mM $MgCl_2$ and 1 mM dithiothreitol at 37°C for 2 h. Then the slides were washed three times with DDW for 5 min each. To detect the sites of non-methylated CCGG sequence of DNA, TdT reaction just similar to that of TUNEL was conducted with 0.5 μM biotin-16-dUTP or 0.5 μM digoxigenin-11-dUTP at 37°C for 1.5 h in a moist chamber and then washed three times with PBS for 5 min each. To visualize the signal, in the case of enzyme immunohistochemistry, the slides were incubated with a mixture of 500 μg/ml of normal goat IgG or normal sheep IgG and 5% BSA in PBS for 1 h and then reacted with HRP-goat anti-biotin or HRP-sheep anti-digoxigenin dissolved in 5% BSA in PBS for 1 h, respectively. After washing with 0.075% Brij in PBS three times and then PBS alone for 10 min each, the signals were visualized with a chromogen solution consisting of DAB, $H_2O_2$, nickel and cobalt ions, as described above. The slides were dehydrated through serial ethanol solutions and cleared by xylene, and then mounted with Permount. In the case of fluorescence immunohistochemistry, FITC-goat anti-biotin or rhodamine-sheep anti-digoxigenin dissolved in 5% BSA in

PBS was reacted for 1 h and washed similarly. The slides were mounted with 90% (v/v) glycerol in PBS.

To detect the sites of methylated CCGG sequence of DNA, the sections were digested with *Hpa* II, then blocked with a mixture of dideoxynucleotides by TdT, as described above. Then, they were fixed with 4% PFA in PBS for 5 min, and washed twice with PBS for 15 min each. After washing with DDW, the sections were digested with 100 units/ml *Msp* I dissolved in Tris/HCl buffer, pH 7.9, containing 10 mM MgCl$_2$, 0.5 mM dithiothreitol, 66 mM potassium acetate and 0.1% BSA at 37°C for 2 h. After washing three times with DDW for 5 min each, TdT reaction was conducted with 0.5 μM biotin-16-dUTP or 0.5 μM digoxigenin-11-dUTP for 37°C for 2 h in a moist chamber and then washed three times with PBS for 5 min each. Then, the same procedures to that used for the detection of non-methylated CCGG sites were taken to visualize the methylated CCGG sites.

For double staining of non-methylated and methylated sites, the *Hpa* II cutting sites were labeled with biotin-16-dUTP by TdT reaction and blocked with dideoxynucleotides. Then, the procedure to detect methylated sites was taken and the *Msp* I cutting sites were labeled with digoxigenin-11-dUTP by TdT reaction. Finally, both haptens were visualized by FITC-anti-biotin and rhodamine-anti-digoxigenin, respectively.

The analysis of fluorescence signals was performed with LSM 5 Pascal (V3.2) (Carl Zeiss Co., Jena, Germany). In this study, FITC and rhodamine signals were obtained with an emission filter of 505-530 nm (excitation; 488 nm) and ~560 nm filter (excitation; 543 nm), respectively. The observation was done with Plan-Neofluar

20 x /0.5 and 40 x /0.75 objective lenses, where optical section thickness was 0.5 and

0.7 μm, respectively.

*Control experiments for HELMET:*

To confirm the specificity of the signals, we conducted several control experiments.

Blocking of 3'-OH ends with dideoxynucleotides before and after *Hpa* II digestion

was essential and assessed by TdT reaction with biotin-16-dUTP or digoxigenin-11-

dUTP. To examine the dependency of signals upon endonuclease activity, some slides

were reacted with the enzyme solution which was kept in a boiling water bath for 10

min and chilled. As a control of TdT reaction, some were reacted without TdT or with

TTP instead of biotin-16-dUTP or digoxigenin-11-dUTP in the reaction mixture. And

some slides were processed omitting HRP- or fluorescent dye-conjugated antibody in

the step of immunohistochemistry to assess endogenous peroxidase activity in

enzyme-immunohistochemistry or auto-fluorescence in fluorescence-

immunohistochemistry.

*Double staining for TUNEL and HELMET:*

To correlate TUNEL-positive cells with the state of methylation of CCGG sequence

directly, TUNEL was first conducted on paraffin sections of mouse testis. After TdT

reaction with biotin-16-dUTP, the sections were blocked with dideoxynucleotides as

described above and fixed with 4% PFA in PBS for 5 min. Then the sections were

washed twice with PBS (15 min each) and once with DDW (5 min), and digested with

*Hpa* II or *Msp* I as described in the above procedure. For co-localization with

non-methylated or methylated sites of CCGG, the cutting sites were labeled with

digoxigenin-11-dUTP by TdT and finally, both biotin and digoxigenin moieties were

visualized with FITC-anti-biotin and rhodamine-anti-digoxigenin, respectively, as

described in detail above.

**Results**

*Optimization of various parameters in HELMET*

Basically, this method depends upon the TdT reaction used in TUNEL; the 3'-OH ends of the cutting sites produced by restriction enzymes were labeled with haptenic dUTP analogues by TdT reaction and successively visualized by enzyme-immunohistochemistry or fluorescence-immunohistochemistry. The conditions for TdT reaction, which had been optimized as described previously (Koji 2000; Koji et al. 2001), were used in this protocol. We set up the conditions of the restriction enzymes (concentrations and durations) to maximize the signal intensity. To avoid detection of non-specific breakage of DNA or unnecessary elongation of the 3'-OH ends of DNA, blocking of the 3'-OH ends with dideoxynucleotides for TdT reaction was essential. When we compared the blocking effect using various concentrations (5-20 μM) of ddUTP, ddTTP and ddATP alone or in combination, a complete block for further TdT reaction was accomplished with a mixture of 20 μM ddTTP and 20 μM ddATP (data not shown). Moreover, repeated fixation with 4% PFA in PBS was also effective in reducing unfavorable staining, probably due to reduced unmasking of originally masked DNA in tissue sections (data not shown).

*Simultaneous localization of both non-methylated and methylated CCGG sequences in mouse testis*

To assess the differences in the ratio of non-methylated to methylated CCGG sequence of DNA among different differentiation stages of spermatogenic cells, we

performed simultaneous staining of both CCGG sequences by HELMET. As shown in Fig. 1a and d, *Hpa* II-positive non-methylated CCGG was localized mainly in the nuclei of some large cells (arrows) and elongated spermatids at stages later than step 10-11 (arrowheads) and at less intensity in the nuclei of spermatogonia. On the other hand, the overall staining of *Msp* I-positive methylated CCGG was more intense and most of the germ cells were positive (Fig. 1b, e). However, some of the large cells showed a little or no staining. In merged images (Fig. 1c, f), it was clear that the large cells were yellow or green, indicating equal or predominant presence of non-methylated CCGG. Based on the H&E-stained slides, those large cells were thought to have undergone apoptosis. Accordingly, we decided to double-stain the cells for TUNEL and HELMET.

In addition, we conducted various control experiments; as shown in Fig 1g and h, the 3'-OH ends of DNA were completely blocked with dideoxynucleotides before and after *Hpa* II digestion. Incubation with inactivated endonucleases (Fig. 1i, j) did not give any signals. Moreover, when TdT reaction with TTP instead of biotin-16-dUTP after *Hpa* II digestion (Fig. 1k) or digoxigenin-11-dUTP after *Msp* I digestion (Fig. 1l) was conducted, no signals were detected. Omitting fluorescent dye-conjugated antibodies did not produce any signals (data not shown).

**PLEASE PLACE FIGURE 1 HERE**

*Differential staining of non-methylated and methylated CCGG sites of DNA in adjacent sections of mouse testis*

Using adjacent sections of mouse testis, we compared the enzyme-immunohistochemical staining of TUNEL, non-methylated CCGG sites and methylated CCGG sites. As shown in Fig. 2b, we found some TUNEL-positive cells as apoptotic cells. When sections were labeled with dideoxynucleotides after proteinase digestion, further TdT reaction in TUNEL did not yield any staining (Fig. 2c). Next, sections that were blocked with dideoxynucleotides were digested with *Hpa* II and the non-methylated CCGG sites were labeled with digoxigenin-11-dUTP by TdT and visualized with HRP-anti-digoxigenin (Fig. 2d). Although the majority of germ cells were only stained very weakly, several cells with strong staining were also noted, which were identified as TUNEL-positive cells. To detect methylated CCGG sites, an adjacent section was digested with *Hpa* II and blocked with dideoxynucleotides, then digested with *Msp* I, labeled with digoxigenin-11-dUTP by TdT and visualized with HRP-anti-digoxigenin (Fig. 2f). Although the majority of germ cells were positive, the intensity of the staining varied among germ cells; some spermatogonia, spermatocytes undergoing cell division and spermatids (round and elongated) were intensely stained. The nuclei of Sertoli cells were only faintly stained except for the nucleoli. Interestingly, unlike the staining of non-methylated CCGG sites, the staining of methylated CCGG sites in some TUNEL-positive cells was very weak. The control sections, in which no *Msp* I digestion was conducted, showed no staining (Fig. 2e), indicating that blockade with dideoxynucleotides was perfect after *Hpa* II digestion. In addition, when TUNEL was performed with TTP instead of biotin-16-dUTP or without TdT, no staining was detected (data not shown).

**PLEASE PLACE FIGURE 2 HERE**

To clarify the state of methylation of CCGG sites in TUNEL-positive cells directly, double staining of TUNEL and *Hpa* II cutting sites or *Msp* I cutting sites was performed. As shown in Fig. 3, TUNEL-positive cells were always positive for *Hpa* II cutting sites (non-methylated CCGG) (Fig. 3c), but not always positive for *Msp* I cutting sites (methylated CCGG) (Fig. 3f).

**PLEASE PLACE FIGURE 3 HERE**

*Immunohistochemical detection of 5-methylcytosine in mouse testis:*

For comparison of the localization pattern of methylated CCGG detected by HELMET with that of 5-methylcytosine, we conducted immunohistochemistry using anti-5-methyl cytosine monoclonal antibody. As shown in Fig. 4a, the nuclei of most germ cells were strongly stained and there was no remarkable difference in the intensity of the staining among germ cells at various differentiation stages. Furthermore, immunohistochemistry for 5-methylcytosine in sections of DES-treated testis showed heavy nuclear staining of germ cells (Fig. 4b) but no difference between TUNEL-positive cells and TUNEL-negative cells (Fig. 4c).

**PLEASE PLACE FIGURE 4 HERE**

**Discussion**

In the present study, we described a new histochemical method, HELMET, designed to discriminate non-methylated and methylated CCGG sequences in tissue sections. The new method HELMET was applied for analysis of paraffin-embedded sections of mouse testes, and the results revealed differences in the level of methylation of CCGG sites that were dependent upon the stage of germ cell differentiation, unlike the results of immunohistochemistry for 5-methylcytosine. Moreover, the results showed that the CCGG sites in TUNEL-positive germ cells, which were mostly undergoing apoptosis, were more or less demethylated, compared with normal germ cells. This is the first direct evidence for the possible involvement of a disorder of epigenetic regulation in the induction of germ cell apoptosis.

Although demethylation of CCGG sites was also found in elongated spermatids at stages later than step 10-11, the most prominent demethylation of CCGG sites was found in TUNEL-positive cells. Since the chromatin is highly condensed in both elongated spermatids and apoptotic cells, methylation of CCGG sites might not be tightly associated with heterochromatin formation. Rather, more importantly, the down-regulation of methylation of CCGG sites may be a possible trigger of induction of germ cell apoptosis in premeiotic germ cells. In agreement with our findings, it is already known that treatment with 5-aza-2'-deoxycytidine (Kelly et al. 2003) and mutation of Dnmt3L gene (Hata et al. 2006), both of which induce a reduction or loss of DNA methylation in mouse testis, resulted in histological anomalies and germ cell loss in mouse testis.

The present results also indicated that the level of methylation at CCGG sites in germ cells was generally higher than that in somatic cells like Sertoli cells. In this context, it should be noted that CpG islands are usually devoid of methylation, and that in other parts of genomic DNA, the methylation level correlates inversely with GC contents in somatic cells. Recent studies, however, reported that the DNA methylation level in germ cells depends upon GC contents of DNA segments (Oakes et al. 2007). Therefore, the generally intense staining of germ cells by HELMET may reflect this tendency. Moreover, it was interesting to find that the CCGG sites of apoptotic germ cells were demethylated during apoptosis, because the mechanism that induces demethylation is not known yet. Our germ cell research might provide important evidence for the presence of a "demethylase".

Generally, hypermethylation of DNA is considered to be associated with heterochromatin formation (Li 2002). However, hypomethylation of CCGG sites was unexpectedly found in the nuclei of elongated spermatids, which are considered to have highly condensed chromatin (Koji and Hishikawa 2003). Further studies are needed to determine whether or how the level of methylation of CCGG sites is closely linked with the heterochromatin area. To confirm this point, such studies should also involve the use of electron microscopy to determine the methylation state of CCGG sites in heterochromatin area.

CpG methylation occurs at $3 \times 10^{7}$ sites throughout the mammalian genome, and the CCGG sites that were analyzed by HELMET constitute at most about 5% of the total number of CpGs that become methylated (Kelly et al. 2003). Therefore, it is not surprising that HELMET allowed us to detect hypomethylation in apoptotic germ

cells, though immunohistochemistry of 5-methylcytosine failed to identify differences in the methylation level between apoptotic and non-apoptotic germ cells. More importantly, the use of isochizomer restriction enzymes, *Hpa* II and *Msp* I, can provide information on methylation of more specific sites of DNA. By extending this method to the use of different combinations of restriction enzymes or by applying this method to specimens in which a specific gene part is hybridized *in situ* with an oligodeoxynucleotide probe (Koji and Nakane 1996), it would be possible to analyze the methylation status of a specific gene in individual cells.

**Acknowledgments**

# References

Allan DJ, Harmon BV, Roberts SA (1992) Spermatogonial apoptosis has three morphologically recognizable phases and shows no circadian rhythm during normal spermatogenesis in the rat. Cell Prolif 25: 241-250

An S, Hishikawa Y, Koji T (2005) Induction of cell death in rat small intestine by ischemia reperfusion: differential roles of Fas/Fas ligand and Bcl-2/Bax systems depending upon cell types. Histochem Cell Biol 123: 249-261

Anway MD, Cupp AS, Uzumcu M, Skinner MK (2005) Epigenetic transgenerational actions of endocrine disruptors and male fertility. Science 308:1466-1469

Bellve AR, Millette CF, Bhatnagar YM, O'Brien DA (1977) Dissociation of the mouse testis and characterization of isolated spermatogenic cells. Histochem Cytochem 25: 480-494

Bourc'his D, Bestor TH (2004) Meiotic catastrophe and retrotransposon reactivation in male germ cells lacking Dnmt3L. Nature 431: 96-99

Bourc'his D, Xu GL, Lin CS, Bollman B, Bestor TH (2001) Dnmt3L and the establishment of maternal genomic imprints. Science 294:2536-2539

Gavrieli Y, Sherman Y, Ben-Sasson SA (1992) Identification of programmed cell death in situ via specific labeling of nuclear DNA fragmentation. J Cell Biol 119: 493-501

Hata K, Okano M, Lei H, Li E (2002) Dnmt3L cooperates with the Dnmt3 family of de novo DNA methyltransferases to establish maternal imprints in mice. Development 129: 1983-1993

Hata K, Kusumi M, Yokomine T, Li E, Sasaki H (2006) Meiotic and epigenetic aberrations in Dnmt3L-deficient male germ cells. Mol Reprod Dev 73: 116-122

Huckins C (1978) The morphology and kinetics of spermatogonial degeneration in normal adult rats: an analysis using a simplified classification of the germinal epithelium. Anat

Rec 190: 905-926

Johnson L, Petty CS, Neaves WB (1983) Further quantification of human spermatogenesis: germ cell loss during postprophase of meiosis and its relationship to daily sperm production. Biol Reprod 29: 207-215

Kelly TL, Li E, Trasler JM (2003) 5-aza-2'-deoxycytidine induces alterations in murine spermatogenesis and pregnancy outcome. J Androl 24: 822-830

Koji T (2000) Molecular Histochemical Techniques (Springer Lab Manuals), Springer-Verlag, Heidelberg

Koji T, Hishikawa Y (2003) Germ cell apoptosis and its molecular trigger in mouse testes. Arch Histol Cytol 66: 1-16

Koji T, Nakane PK (1996) Recent advances in molecular histochemical techniques: in situ hybridization and southwestern histochemistry. J Electron Microsc 45: 119-127

Koji T, Hishikawa Y, Ando H, Nakanishi Y, Kobayashi N (2001) Expression of Fas and Fas ligand in normal and ischemia-reperfusion testes: Involvement of the Fas system in the induction of germ cell apoptosis in the damaged mouse testis. Biol Reprod 64: 946-954

Li E (2002) Chromatin modification and epigenetic reprogramming in mammalian development. Nat Rev Genet 3: 662-673

Li JY, Lees-Murdock DJ, Xu GL, Walsh CP (2004) Timing of establishment of paternal methylation imprints in the mouse. Genomics 84:952-960

Matsuo Y, Nomata K, Eguchi J, Aoki D, Hayashi T, Hishikawa Y, Kanetake H, Shibata Y, Koji T (2007) Immunohistochemical analysis of connexin43 expression in infertile human testes. Acta Histochem Cytochem 40: 69-75

Oakberg EF (1956) A description of spermiogenesis in the mouse and its use in analysis of the cycle of the seminiferous epithelium and germ cell renewal. Am J Anat 99: 391-413

Oakes CC, La Salle S, Smiraglia DJ, Robaire B, Trasler JM (2007) A unique configuration of genome-wide DNA methylation patterns in the testis. Proc Natl Acad Sci USA 104: 228-233

Reik W, Dean W, Walter J (2001) Epigenetic reprogramming in mammalian development. Science 293: 1089-1093

Shukuwa K, Izumi S, Hishikawa Y, Ejima K, Inoue S, Muramatsu M, Ouchi Y, Kitaoka T, Koji T (2006) Diethylstilbestrol increases the density of prolactin cells in male mouse pituitary by inducing proliferation of prolactin cells and transdifferentiation of gonadotropic cells. Histochem Cell Biol 126: 111-123

Wang RA, Nakane PK, Koji T (1998) Autonomous cell death of mouse male germ cells during fetal and postnatal period. Biol Reprod 58: 1250-1256

Yamazaki Y, Mann MR, Lee SS, Marh J, McCarrey JR, Yanagimachi R, Bartolomei MS (2003) Reprogramming of primordial germ cells begins before migration into the genital ridge, making these cells inadequate donors for reproductive cloning. Proc Natl Acad Sci USA 100:12207-12212

**Figure legends**

**Fig. 1** Simultaneous localization of non-methylated and methylated CCGG sequences by HELMET in a paraffin-embedded section of mouse testis.

The paraffin-embedded section was blocked with a dideoxynucleotide mixture by TdT and then the *Hpa* II cutting sites were labeled with biotin-16-dUTP. After dideoxynucleotide blockade, *Msp* I cutting sites were labeled with digoxigenin-11-dUTP and then both haptens were visualized with FITC-anti-biotin (**a, d**) and rhodamine-anti-digoxigenin (**b, e**), respectively. Merged images are shown in (**c**) and (**f**). *Arrows* a large cell, *arrowheads* elongated spermatids. As controls, various experiments were conducted. **g** Blockade of 3'-OH ends with dideoxynucleotides by TdT. The TdT reaction with biotin-16-dUTP was conducted on a section just after the blockade with dideoxynucleotides, and followed by the reaction with FITC-anti-biotin. No staining was found. **h** Blockade of *Hpa* II cutting sites with dideoxynucleotides by TdT. A section was digested with *Hpa* II, and blocked with dideoxynucleotides by TdT. Then the section was processed similarly to (**g**). No staining was found. As further controls, boiled (inactivated) *Hpa* II (**i**) or *Msp* I (**j**) was reacted with a section after the blockade with dideoxynucleotides and then the TdT reaction with biotin-16-dUTP or digoxigenin-11-dUTP, respectively, was done. The signal was detected with FITC-anti-biotin and rhodamine-anti-digoxigenin.   No staining was found. As a control of TdT reaction, the reaction was conducted with TTP in place of biotin-16-dUTP after *Hpa* II digestion (**k**) or digoxigenin-11-dUTP after *Msp* I digestion (**l**) in HELMET. No fluorescence was found. **a, b, c, g, h, i, j, k, l** *Bar*=100

μm, **d**, **e**, **f** *Bar*=50 μm.


**Fig. 2** Methylation level of CCGG sites in TUNEL-positive germ cells in adjacent

sections of mouse testis.

      Adjacent sections of paraffin-embedded mouse testis were used for H&E

staining, TUNEL, non-methylated CCGG sites and methylated CCGG sites, as

described in detail in "Materials and methods". **a** H&E staining. **b** TUNEL staining. **c**

Blockade of 3'-OH ends with dideoxynucleotides by TdT. After blockade, the section

was labeled with biotin-16-dUTP by TdT and the incorporated biotin was detected

with HRP-anti-biotin. No signals were observed. **d** Staining for non-methylated

CCGG sites. After the blockade procedure described in (**c**), the section was digested

with *Hpa* II, labeled with biotin-16-dUTP and visualized by

enzyme-immunohistochemistry with HRP-anti-biotin. **e** Blockade of *Hpa* II cutting

sites with dideoxynucleotides by TdT. The section was digested with *Hpa* II and the

cutting sites were blocked with a dideoxynucleotide mixture. Then the section was

processed in a manner similar to that described in (**c**). **f** Staining for methylated

CCGG sites. After blockade of *Hpa* II cutting sites with dideoxynucleotides, the

section was digested with *Msp* I and the cutting sites were labeled with

biotin-16-dUTP and visualized with HRP-anti-biotin. *Bar*=100 μm.


**Fig. 3** Double staining of TUNEL and non-methylated CCGG sites or methylated

CCGG sites in paraffin-embedded sections of mouse testis.

Paraffin-embedded sections of mouse testis were first processed for TUNEL with biotin-16-dUTP to detect apoptotic cells, followed by blockade with dideoxynucleotides by TdT. Then the sections were digested with *Hpa* II or *Msp* I and the cutting sites were labeled with digoxigenin-11-dUTP by TdT. Finally, biotin and digoxigenin moieties were detected by FITC anti-biotin and rhodamine anti-digoxigenin, respectively. (**a**, **d**) TUNEL staining. **b** Staining for *Hpa* II cutting sites (non-methylated CCGG sites). **c** A merged image of (**a**) and (**b**). **e** Staining for *Msp* I cutting sites (methylated CCGG sites). **f** A merged image of d and e. *Bar*=100 μm. *Arrows* (**a**, **b** and **c**) or *arrow heads* (**d**, **e** and **f**) indicate the same cell.

**Fig. 4**: Immunohistochemical detection of 5-methylcytosine in paraffin-embedded sections of DES treated mouse testis.

Paraffin-embedded sections of corn oil (**a**)- or DES (**b**)-treated mouse testis, as described in "Materials and methods", were reacted with anti-5-methylcytosine antibody and the signals were detected by enzyme-immunohistochemistry. The mirror section of that used for (**b**) was used for TUNEL (**c**). *Arrows* in (**b**) indicate the cells which are identical with the TUNEL positive cells indicated by *arrows* in (**c**). *Bar*=100 μm.
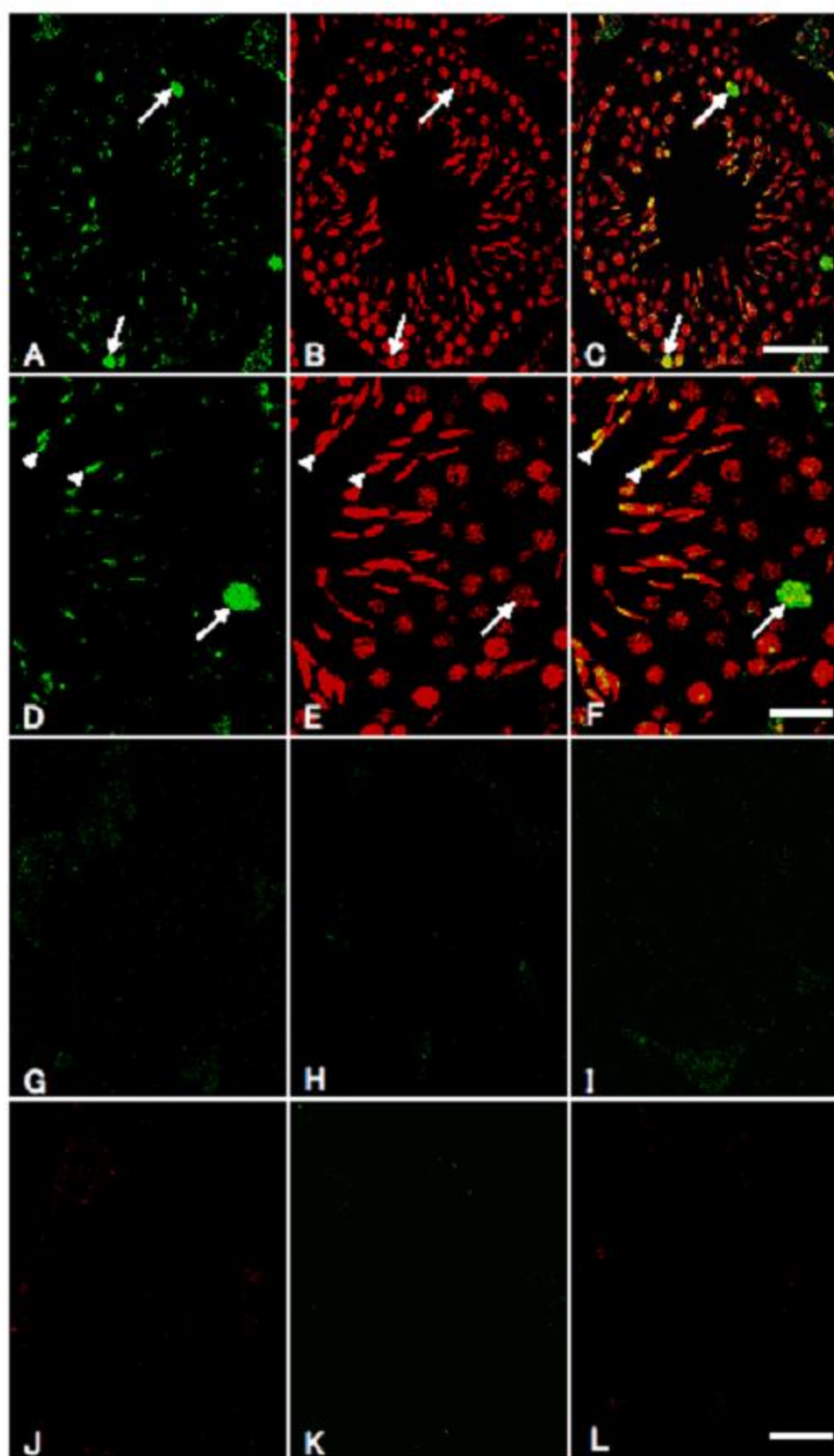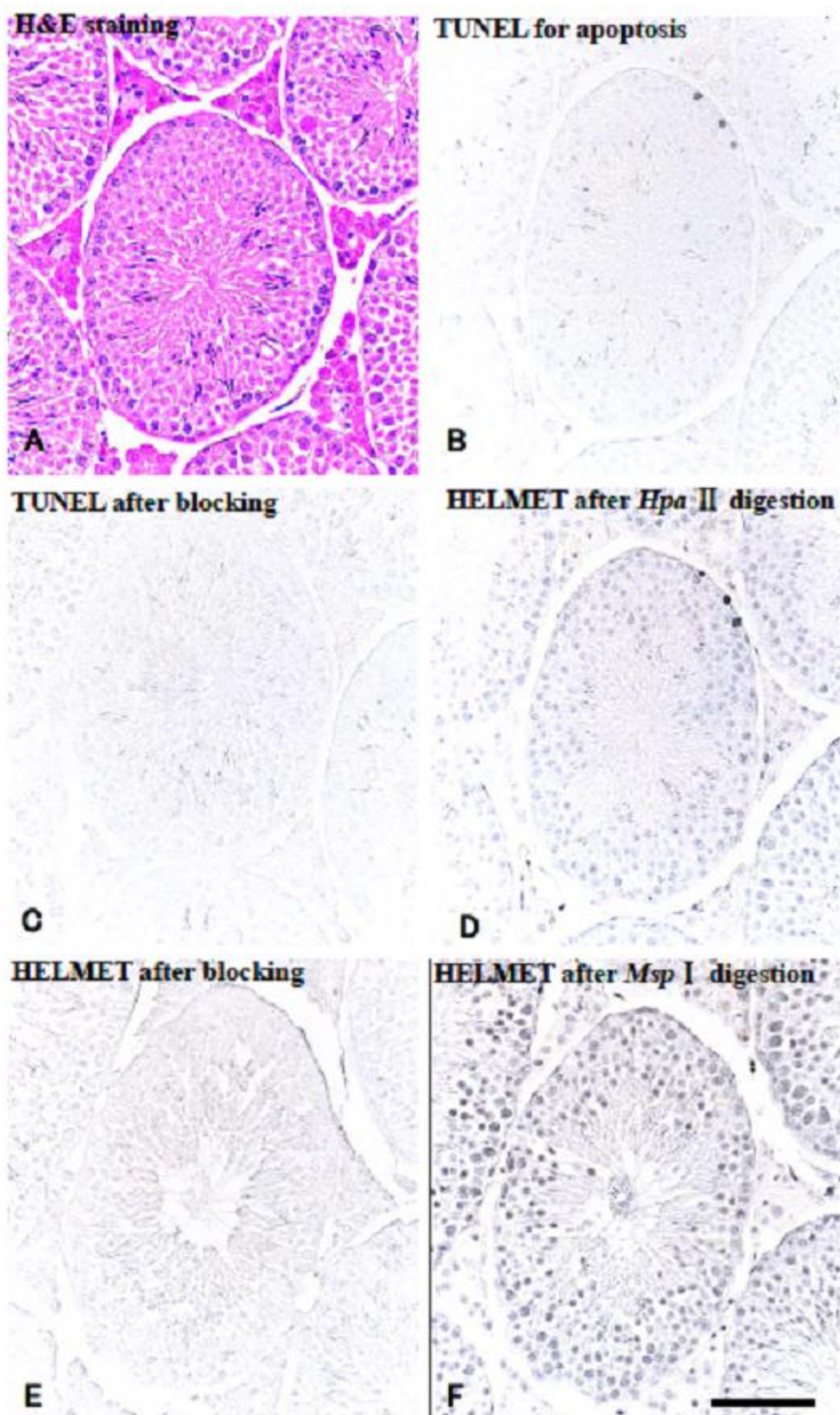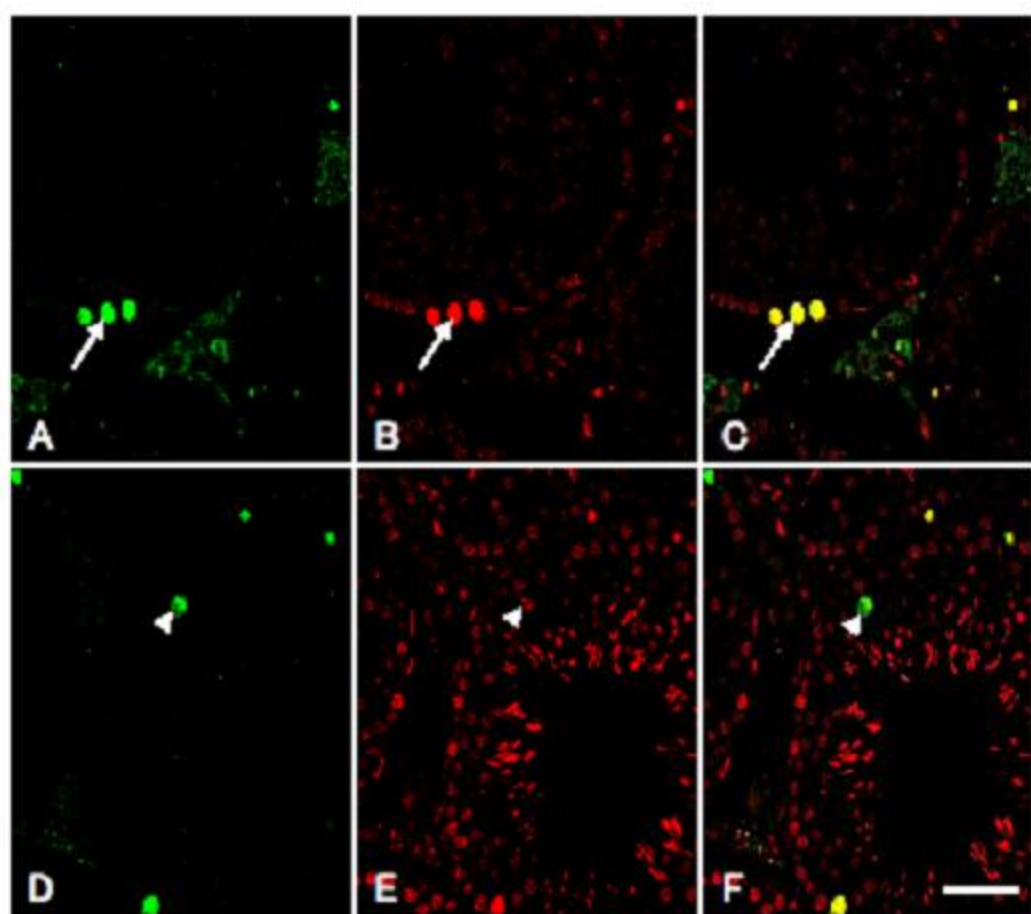
Fig 1

# Fig 2



**A** — H&E staining
**B** — TUNEL for apoptosis
**C** — TUNEL after blocking
**D** — HELMET after *Hpa* II digestion
**E** — HELMET after blocking
**F** — HELMET after *Msp* I digestion

# Fig 3

# Fig 4